Revision 1

Word counts: 5920 (Abstract, full text, and figure captions)

Ultrasonic Studies of alkali-rich hydrous silicate glasses: elasticity, density, and implications for water dissolution mechanisms

Bohan Liu[1], Qiong Liu[1,*], Baosheng Li[2], Harald Behrens[3], Rebecca A. Lange[4]

[1] Key Laboratory of Orogenic Belts and Crustal Evolution, MOE, School of Earth and Space Science, Peking University, Beijing 100871, P.R. China.

[2] Department of Geosciences, Stony Brook University, Stony Brook, New York 11794, U.S.A

[3] Institute of Mineralogy, Leibniz University Hannover, Callinstr. 3, D-30167 Hannover, Germany

[4] Department of Earth and Environmental Sciences, University of Michigan, 2534 C.C. Little Building, 1100 North University Avenue, Ann Arbor, Michigan 48109-1005, USA

*Corresponding author:

Email: qiong.liu@pku.edu.cn

This is the peer-reviewed, final accepted version for American Mineralogist, published by the Mineralogical Society of America.
The published version is subject to change. Cite as Authors (Year) Title. American Mineralogist, in press.
DOI: https://doi.org/10.2138/am-2022-8451. http://www.minsocam.org/

Abstract

The acoustic velocities of three series of alkali-rich hydrous silicate glasses were determined at ambient conditions using ultrasonic interferometry. The sound velocities and calculated elastic properties are nearly linear functions of dissolved water content. The water content derivatives of both compressional ($\partial(V_P)/\partial(X_{H_2O})$) and shear wave velocity ($\partial(V_S)/\partial(X_{H_2O})$) decrease with increasing Na_2O content, which suggests that increasing sodium content might weaken the effect of water on acoustic velocities. For each glass series, the shear modulus decreases with increasing water content, whereas the adiabatic bulk modulus (K_S) varies little with water content. By comparing our results of K_S to previously published data on hydrous felsic alkalic (rhyolite, phonolite, and trachyte) glasses, we speculate that H_2O may have a negligible effect on the compressibility of felsic alkalic glasses/melts. The measured densities of each series of glasses were converted to molar volumes and extrapolated to the hypothetical pure water to derive the partial molar volume of water ($\bar{V}_{H_2O}$). The resulting $\bar{V}_{H_2O}$ was found to be independent of composition, with a value of 10.4 ± 0.5 cm^3/mol at room temperature. Whereas the partial molar bulk modulus (K_S) of water is composition-dependent. Furthermore, the Poisson's ratio (v) increases with increasing water content for all three composition series. Therefore, the similar behavior of Al-free and Al-bearing glasses implies that water depolymerizes melts in both systems. The decrease of water content derivative of the Poisson's ratio ($\partial(v)/\partial(X_{H_2O})$) with increasing Al/(Al + Si) (Q^4(4Al) accordingly)

indicates that water interaction with Al-O bonds to produce Al-OH depolymerizes peralkaline silicate melts less effectively than with Si-O bonds to form Si-OH. Hence, we speculate that water prefers to interact with Si-O bonds rather than Al-O bonds in peralkaline silicate systems. The dissolution mechanisms of water between peraluminous and peralkaline melts might be different, which merits further research.

Keywords: ultrasonic interferometry, hydrous silicate glasses, alkali-rich, the partial molar volume of water, elastic properties, water speciation; dissolution mechanisms

This is the peer-reviewed, final accepted version for American Mineralogist, published by the Mineralogical Society of America.
The published version is subject to change. Cite as Authors (Year) Title. American Mineralogist, in press.
DOI: https://doi.org/10.2138/am-2022-8451. http://www.minsocam.org/

47 ## Introduction

48

49 The presence of water in magmas has long been considered an important control of
50 igneous activities. Water is the most dominant volatile constituent of natural magmas and
51 plays a dramatic role in the physicochemical properties of silicate melts and glasses. For
52 instance, the density and the partial molar volume of water ($\bar{V}_{H_2O}$) of hydrous silicate
53 melts have been studied *in-situ* using various methods, including the *P-V-T* cell in two
54 interconnected internally heated pressure vessels (Burnham and Davis 1971), X-ray
55 absorption (Malfait et al. 2014a, 2014b; Sakamaki et al. 2009; Seifert et al. 2013), and the
56 sink-float method (Agee 2008; Jing and Karato, 2012; Matsukage et al. 2005; Sakamaki
57 et al. 2006). The investigations of hydrous supercooled liquids have provided further
58 constraints on the volumetric characteristics of water dissolved in silicate melts (Ochs
59 and Lange 1997, 1999; Bouhifd et al. 2001, 2015). Furthermore, a review of available
60 density data of hydrous silicate glasses shows that $\bar{V}_{H_2O}$ is independent of composition
61 by the intercept method (Richet et al. 2000). It was further investigated for a range of
62 glasses under ambient conditions using the same method (Ardia et al. 2014; Balzer et al.
63 2020; Wu et al. 2017).

64 Due to the technical difficulties in measurements of melts at crustal or mantle
65 conditions, several ambient condition investigations have focused on silicate glasses to
66 deduce the structure and behavior of silicate melts. The pronounced effects of H_2O on

This is the peer-reviewed, final accepted version for American Mineralogist, published by the Mineralogical Society of America.
The published version is subject to change. Cite as Authors (Year) Title. American Mineralogist, in press.
DOI: https://doi.org/10.2138/am-2022-8451. http://www.minsocam.org/

67 silicate glasses could provide some insights into the hydrous melts. Recently, Le Losq et
68 al. (2017) reported that strong hydrogen bonds (H-bonds) are present in Na-bearing
69 glasses below glass transition temperature (T_g) in an *in-situ* Raman spectroscopic study,
70 which indicates glasses are inadequate to describe the structure of the corresponding
71 melts. However, the missing of strong H-bonds in the Ca-bearing glasses indicates that
72 the formation of H-bonds in glasses depends on glass composition. Therefore, further
73 studies on the structure and properties of glasses are needed to understand the similarities
74 and differences between glasses and melts.

75 Understanding the high compressibility for hydrous melts can aid in predicting
76 density increase with depth. Sound velocities are the prime data to provide direct
77 information on the elastic moduli and compressibility. Nevertheless, the effect of
78 dissolved water on the acoustic velocities and elastic behaviors of silicate glasses are still
79 poorly constrained. A few experiments on geological relevant compositions have been
80 conducted by Brillouin spectroscopy at ambient conditions. According to Richet and
81 Polian (1998), the partial molar bulk modulus (K_S) of water in andesite glasses (18 ± 3
82 GPa) is similar to that of Ice VII (23.7 ± 0.9 GPa) (Hemley et al. 1987), suggesting that
83 water behaves as the densest form of ice. The partial molar compressibility of water is
84 shown to be strongly dependent on composition over a range of hydrous silicate glasses
85 (Malfait et al. 2011; Whittington et al. 2012), implying $\bar{V}_{H_2O}$ may be affected by
86 composition at elevated pressures. Wu et al. (2017) showed that the effect of dissolved

87 water on the sound velocities of basalt glasses has tremendous discrepancies with
88 previous studies. Recently, Gu et al. (2021) found that reductions in velocities due to
89 hydration are larger in shear velocity than those in compressional velocity.

90 To better constrain the role of water on acoustic velocity and elasticity, the range of
91 glass compositions needs to be expanded. Many models of water dissolution in silicate
92 systems assume that water ruptures T-O-T links and behaves as a network modifier, much
93 like alkali oxides such as Na_2O (Whittington et al. 2001). In addition, it was
94 demonstrated that alkali oxides and water have similar effects on volume (Richet and
95 Polian 1998; Richet et al. 2000) and viscosity of silicate glasses (Dingwell et al. 1996).
96 However, relationships between the effects of water and alkali oxides have not been
97 revealed by elasticity measurements. Systematic investigations of the elastic behavior are
98 required to clarify the effect of alkali oxides and water on silicate glasses.

99 The main purpose of this study is to constrain the effect of water content on the
100 sound velocities and elastic behaviors of three series of alkali-rich silicate glasses with up
101 to 5.25 wt% H_2O by ultrasonic interferometry at ambient conditions. The feasibility of
102 using this method for the first successful determinations of acoustic velocities on hydrous
103 silicate glasses is presented. Another goal of this study is to investigate whether $\overline{V}_{H_2O}$ in
104 silicate glasses depends on composition at room temperature. The dependence of the
105 partial molar K_S and volume of water on compositions in silicate glasses and melts are
106 compared and the causes for their contrasting behaviors are explained. Moreover, two

This is the peer-reviewed, final accepted version for American Mineralogist, published by the Mineralogical Society of America.
The published version is subject to change. Cite as Authors (Year) Title. American Mineralogist, in press.
DOI: https://doi.org/10.2138/am-2022-8451. http://www.minsocam.org/

107 possible interpretations are proposed for linear functions of physical properties with
108 water content based on water speciation. Finally, the Poisson's ratio and its water content
109 derivative ($\partial(v)/\partial(X_{H_2O})$) are used to infer the dissolution mechanisms of water.
110
111 ## Experimental methods
112
113 ### Synthesis of hydrous glasses
114 Three anhydrous alkali-rich multicomponent silicate glasses (Nelson9, Nelson15,
115 and NAS15) were selected as the starting materials, which were originally synthesized by
116 Nelson and Carmichael (1979) and Riebling (1966) (please refer to the two papers for
117 details). We only give a brief description of synthesis procedures here. Reagent grade
118 oxide and carbonate powders were weighed in the proportions required and then fused in
119 Pt crucibles at 1500-1700°C in a box furnace. After a few hours, the melts were poured
120 on graphite plates and quenched to glasses. Repeated cycles of grinding and fusion were
121 implemented to ensure homogeneity of the glasses. The nominal compositions of three
122 anhydrous glasses are listed in Table 1. All the starting materials used in this work were
123 remelted to drive off the adsorbed water and ground into powder.
124 For each starting material, 3-5 hydrous specimens containing different amounts
125 (0-5.45 wt%) of water were synthesized (See Behrens et al. 1996 for a detailed
126 description). Briefly, the samples were hydrated by sealing powdered glasses and

distilled water in platinum capsules, which were welded shut and isostatically hot pressed under hyperliquidus conditions at 5 kbar and 1507-1673 K for a few hours in internally-heated gas pressure vessels. The power supply was turned off at the end of the experiments, and the glasses were quenched isobarically to prevent the formation of bubbles and water exsolution. The recovered run products used in this study were quenched to homogeneous glasses, free of crystals and bubbles, at least to the resolution of optical microscopy.

Characterization of hydrous glasses

The water contents were determined by Karl Fischer Titration (KFT) analysis (Table 1), with the apparatus and procedures described by Behrens (1995) and Holtz et al. (1992). The hydrous glasses were rapidly heated up in a Pt sample holder using a high-frequency generator. The released H_2O was transported with a pre-dried argon stream to the titration cell, where the water content was quantified based on the reaction with coulometrically generated iodine and chemically bound sulfur dioxide already present. To check the homogeneity of dissolved water distribution within silicate glasses, thin slices cut from both ends of several recovered sample cylinders were analyzed. The uncertainty on the reported water content is typically smaller than 0.1 wt%. Although the amounts of dissolved water were not measured after sound velocity experiments, there is no reason to believe that water was lost during the measurements at ambient conditions.

147 The chemical compositions of samples were determined by electron microprobe
148 analyses (EMPA), and the reported values are averages of at least 10-point analysis
149 (Table 1). Morgan and London (1996, 2005) proposed that sodium (Na) migration is
150 more evident in hydrous alkali aluminosilicate glasses than in anhydrous ones. To
151 minimize alkali mobilization, the EMPA was performed on a Jeol JXA-8230 with 15 kV
152 acceleration voltage, 5 nA beam current, and 30 μm diameter defocused beam.

153 The densities (ρ) of samples were further characterized by the Archimedean method
154 at room temperature (298 K). Each glass was weighed 5–15 times with an electronic
155 analytical balance (METTLER TOLEDO XS204) in air and while immersed in toluene.
156 The density is expressed as $\rho = \frac{m_1}{m_1 - m_2}\rho_0$, where ρ_0 is the known density of toluene;
157 m_1 and m_2 are the measured weights of investigated silicate glasses in air and toluene.

158

159 **Ultrasonic interferometry: transfer function method**

160 The ultrasonic experiments were conducted using the ultrasonic interferometry
161 system at Peking University. Ultrasonic interferometry combined with the transfer
162 function method was used to determine the round-trip travel times of ultrasonic waves
163 through the specimens. A detailed description of the transfer function technique can be
164 found elsewhere (Li et al. 2002, 2004). The pure-mode longitudinal (Z-cut) and shear (41°
165 X-cut) $LiNbO_3$ piezoelectric transducers were used to measure travel times ($t_{(P,S)}$),
166 respectively. The longitudinal (V_P) and transverse sound velocity (V_S) can be calculated

with measured travel time ($t_{(P,S)}$) and specimen lengths (L) at ambient conditions: $V_{(P,S)} = 2L/t_{(P,S)}$.

The experimental setup for ultrasonic interferometry travel time measurements is shown in Fig. 1. The piezoelectric transducer transmits and receives a broadband radio-frequency (RF) pulse. The propagation time within the specimen is determined by the time delay between two consecutive echoes reflected from the front and back surfaces of the specimen (Fig. 1). With sandpaper and diamond paste, the two surfaces along the acoustic path of each glass were polished to be optically flat and parallel. The transfer function method of ultrasonic interferometry allows rapid collection of real-time acoustic data (Fig. 2a) and subsequent analysis offline (Li and Liebermann 2007). After that, sine wave tone bursts (30 MHz, 10 cycles for longitudinal wave and 20 MHz, 5 cycles for transverse wave) are used to convolute with the transfer function to simulate pulse-echo overlap (PEO) measurement. Finally, the travel time is determined by shifting the second copy relative to the initial echo pattern until the specimen echo and buffer rod echo overlap (Fig. 2b).

Experimental precision and accuracy

Measurements were first carried out on a working standard (fused silica), whose sound velocity and density have been determined previously by other techniques, to check the accuracy of all facilities before measuring samples (Table 2). Our results are

187 consistent with available data (Andreatch and McSkimin 1976; Meister et al. 1980;
188 Manghnani et al. 2020) and the average error in the velocity and density measurements
189 are about 0.34% and 0.07%, respectively. In addition, the measurements of water-free
190 andesite glass (chemical composition presented in Table 1) compare well with data from
191 the literature with similar compositions (Table 2). The excellent agreement enables us to
192 provide a well-defined constraint on the role of H_2O on the elastic properties of
193 alkali-rich silicate glasses. The reported precisions of measured values are obtained as the
194 mean standards deviation from repetitive measurements, while errors of derived values
195 are calculated by propagating experimental uncertainties (Table 3).
196
197 **Results**
198
199 The measured densities, lengths, travel times of alkali-rich hydrous silicate glasses
200 are reported in Table 3. Within experimental uncertainty, the density of each glass series
201 shows a linear dependence on the water content (Fig. 3). The decrease in glass density
202 with the addition of H_2O can be attributed to the low atomic mass of hydrogen, which
203 causes the H_2O component dissolved in glass to be much less dense than other oxide
204 components. Density is reduced by 0.3%, 0.43%, and 0.53% for Nelson9, Nelson15, and
205 NAS15 respectively when H_2O is increased by 1 wt%. In addition, the density decreases

This is the peer-reviewed, final accepted version for American Mineralogist, published by the Mineralogical Society of America.
The published version is subject to change. Cite as Authors (Year) Title. American Mineralogist, in press.
DOI: https://doi.org/10.2138/am-2022-8451. http://www.minsocam.org/

206 with increasing SiO_2 content over the composition range investigated ($\rho_{Nelson9} <$
207 $\rho_{Nelson15} < \rho_{NAS15}$, Fig. 3).

208 The acoustic velocities are plotted against water content in Fig. 4. For Nelson9
209 glasses, V_P and V_S decrease at the rate of 8.2 and 12.3 m/s per mol% dissolved H_2O,
210 respectively. For Nelson15 glasses (0-9.89 mol% H_2O), V_P decreases from 5813 to 5781
211 m/s and V_S decreases from 3484 to 3423 m/s. For NAS15 glasses, the data suggest that V_S
212 decreases slightly with increasing dissolved H_2O, whereas V_P is virtually independent of
213 dissolved H_2O. An important feature of Fig. 4 is the lack of a systematic behavior of the
214 variation of V_P and V_S with water content in various compositions.

215 The adiabatic bulk modulus (K_S) is derived from the measured density and sound
216 velocities: $K_s = \rho \cdot \left({V_P}^2 - 4/3\,{V_S}^2\right)$. According to the equation: $G = \rho \cdot {V_s}^2$, the shear
217 modulus (G) magnifies the variations of the shear velocity. As shown in Fig. 5, the shear
218 moduli for all three series decrease with increasing dissolved H_2O. However, dissolved
219 water has no discernible effect on the bulk modulus of alkali-rich silicate glasses. The
220 effect of chemical composition on K_S is more obvious than on G. For instance, the bulk
221 and shear modulus increase from 39 to 48 (23.1%) and 26 to 30 (15.4%) GPa for
222 anhydrous glasses, respectively.

223 The molar volume (V) was calculated from the gram formula weight (*g.f.w.*) and
224 density: $V = g.f.w./\rho$ (Table 3). The dependence of the molar volume on dissolved
225 H_2O is found to be linear with a low degree of scattering (Fig. 6a).

This is the peer-reviewed, final accepted version for American Mineralogist, published by the Mineralogical Society of America.
The published version is subject to change. Cite as Authors (Year) Title. American Mineralogist, in press.
DOI: https://doi.org/10.2138/am-2022-8451. http://www.minsocam.org/

226

227 # Discussion

228

229 ## The effect of water on wave velocities and elastic moduli

230 The different trend in wave velocities is likely attributed to the different Na_2O
231 content. For instance, it appears that the water content derivatives of the shear
232 $(\partial(V_S)/\partial(X_{H_2O}))$ and compressional wave velocity $(\partial(V_P)/\partial(X_{H_2O}))$ decrease with
233 increasing Na_2O content (Fig. 4, Table 4). This implies that the increase in sodium
234 content might diminish the influence of water on acoustic velocities. For each
235 composition, the effect of increasing water content on acoustic velocities was weaker for
236 V_P than for V_S (Fig. 4, Table 4). The larger decreases in V_S can be ascribed to
237 depolymerization of the silicate network by hydroxyl groups, which reduces its shear
238 resistance (Deschamps et al. 2011). V_P is not affected as much because the
239 compressibility of the glass structure is not influenced as much by H_2O_{mol} in interstitial
240 voids or depolymerization by hydroxyl groups (Gu et al. 2021). The wave velocities of
241 basalt glasses, on the other hand, suggest that dissolved water has a smaller effect on V_S
242 than on V_P (Malfait et al. 2011; Whittington et al. 2012; Wu et al. 2017). This contrasting
243 behavior might be due to water speciation in glasses, which is affected by chemical
244 composition (the degree of polymerization), cooling history (T_g), and temperature
245 (Behrens 2020; Behrens and Yamashita 2008; Le Losq et al. 2015; Nowak and Behrens

246 1995; Romano et al. 1995).

247 The elastic moduli of basalt and andesite glasses systematically decrease as the
248 water content increases (Malfait et al. 2011; Richet and Polian 1998; Whittington et al.
249 2012; Wu et al. 2017). The adiabatic compressibility (β_S) was determined from the
250 relation: $\beta_S = 1/K_S$. Therefore, the addition of water increases compressibility. This
251 suggested that H_2O reacts with the bridging oxygen of tetrahedra in basalt and andesite
252 glasses, resulting in more compressible silicate structures. However, for each series of
253 glasses in this study, the bulk modulus is nearly constant with the addition of H_2O, which
254 is broadly consistent with the elastic behaviors of rhyolite (Malfait et al. 2011), phonolite,
255 and trachyte (Whittington et al. 2012) glasses (Fig. 5a). Likewise, the compressibility is
256 also nearly constant, coinciding with the viewpoint that the H_2O component becomes less
257 compressible with increasing alkalinity (Whittington et al. 2012). The minimal effect of
258 dissolved H_2O on K_S observed in rhyolite glasses was interpreted that V_S decreases more
259 strongly than V_P, which counterbalances the concomitant decrease in density upon
260 hydration (Malfait et al. 2011).

261 According to a prior study, both K_S and G of silicate glasses slightly decrease with
262 increasing SiO_2 concentrations (Malfait et al. 2011). Our observations report the decrease
263 in K_S as silica content increases (Fig. 5a). Nonetheless, the fitted line from the shear
264 moduli of the NAS15 glass series, which have the lowest SiO_2 content, is located in the
265 middle (instead of the upper) range of the three series of glasses (Fig. 5b). This abnormal

266 behavior is most likely attributed to the high Na_2O content (up to 29 wt%) in NAS15
267 glasses. Malfait and Sanchez-valle (2013) demonstrated that bulk modulus is almost
268 independent of Na_2O content, while shear modulus decreases systematically with
269 increasing Na_2O content. Thus, the high Na_2O content in NAS15 glasses might cause the
270 anomaly in shear moduli, but not in bulk moduli.

271 The number of non-bridging oxygens per tetrahedrally coordinated cation (NBO/T)
272 provides a measurement of the degree of polymerization, which is one of the most critical
273 characteristics for controlling magmatic processes in the Earth's interior. Whittington et
274 al. (2012) proposed that acoustic velocity and elastic modulus increase with decreasing
275 degrees of polymerization. This trend obtained from aluminosilicate glasses with a broad
276 range of polymerization does not apply to our samples. For instance, Fig. 4b and Fig. 5b
277 display the opposite trend that shear wave velocity and shear modulus decrease with
278 decreasing polymerization (NBO/T value for anhydrous samples are shown in Table 4).
279 The reason for this may be due in part to the compositions of our samples falling outside
280 the composition range of previous studies, for example, Nelson15 and NAS15 are
281 alkaline-earth-elements-free and Nelson9 is alumina-free. These behaviors appear to be
282 more complex than the previous conclusion. Thus, the trends of sound velocity and
283 elastic modulus on silicate glasses are not independently determined by the SiO_2 content
284 or the degree of polymerization, both or even more factors should be considered. For
285 instance, it is demonstrated that the temperature at which the glass transition takes place

This is the peer-reviewed, final accepted version for American Mineralogist, published by the Mineralogical Society of America.
The published version is subject to change. Cite as Authors (Year) Title. American Mineralogist, in press.
DOI: https://doi.org/10.2138/am-2022-8451. http://www.minsocam.org/

(T_g) affects the densities (hence the elastic properties) of glasses (Richet et al. 2000).

Notably, the elastic moduli of the felsic alkalic (phonolite, trachyte, and rhyolite) glasses derived from Brillouin scattering spectroscopy (Malfait et al. 2011; Whittington et al. 2012) show a similar trend to our results (Fig. 5), with all glasses sharing the common feature of being alkali-rich. These felsic alkalic rocks are a relatively small component of ocean island volcanic suites (Thompson et al. 2001). The role of water in the physicochemical properties of those melts is critical for modeling the magmatic activities at crustal depths (Ardia et al. 2014). If the investigated multicomponent compositions are extrapolated to natural compositions, the observations of this study suggest that water has a negligible effect on bulk modulus and compressibility in felsic alkalic glasses/melts.

The room-temperature partial molar volume of water ($\bar{V}_{H_2O}$) in glasses

By linearly extrapolating molar volume to the hypothetical pure water component, the room-temperature $\bar{V}_{H_2O}$ in glasses can be derived to be 10.0 ± 0.5, 10.6 ± 0.3, and 10.6 ± 0.4 cm^3/mol for Nelson9, Nelson15, and NAS15 glasses, respectively (Table 5). This extrapolation method to obtain $\bar{V}_{H_2O}$ is based on the assumption of ideal mixing between water and the silicate components (Richet et al. 2000). As shown in Fig. 6b, the linear dependence of molar volume on the dissolved water demonstrates that $\bar{V}_{H_2O}$ is independent of composition, which is consistent with the ideal mixing model.

Table 5 displays $\bar{V}_{H_2O}$ and synthesis *P*-*T* conditions in various studies. It appears

This is the peer-reviewed, final accepted version for American Mineralogist, published by the Mineralogical Society of America.
The published version is subject to change. Cite as Authors (Year) Title. American Mineralogist, in press.
DOI: https://doi.org/10.2138/am-2022-8451. http://www.minsocam.org/

306 that $\bar{V}_{H_2O}$ varies with the synthesis pressure. For example, the $\bar{V}_{H_2O}$ values obtained at 2
307 GPa (~9 cm^3/mol) are remarkedly lower than those obtained from 1 GPa runs (~10-11
308 cm^3/mol) (Wu et al. 2017). In contrast, Ardia et al. (2014) showed that the $\bar{V}_{H_2O}$
309 increases to ~14 cm^3/mol at the highest synthesis pressure (2.5 GPa). For the three
310 composition series in this study, $\bar{V}_{H_2O}$ is almost constant at 10.4 ± 0.5 cm^3/mol, which
311 might be attributed to the same synthesis pressure, eliminating the potential effect of
312 synthesis pressure. Due to the large extrapolation to 100 mol% H_2O, the data obtained in
313 this study are considered to be broadly consistent with the constant value of 12.0 ± 0.5
314 cm^3/mol by Richet et al. (2000).

315 From density and thermal expansion measurements on hydrous silicate glasses, it
316 has been reported that $\bar{V}_{H_2O}$ is nearly independent of composition in supercooled liquids
317 near T_g (Ochs and Lange 1997, 1999; Bouhifd et al. 2001, 2015). Malfait et al. (2014a)
318 have combined literature data to conclude that $\bar{V}_{H_2O}$ is independent of composition for
319 silicate melts at simultaneous high *P*-*T* conditions, at least within experimental
320 uncertainties. The constant $\bar{V}_{H_2O}$ in glasses, supercooled liquids, and melts will simplify
321 the construction of a volumetric model for hydrous magmas under geologically relevant
322 conditions.

323

324 **The partial molar bulk modulus of water in glasses and melts**

325 The partial molar volume of water appears to be insensitive to the anhydrous

326 composition for melts as well as glasses, but this is not the case for the partial molar
327 elastic modulus of water. The partial molar bulk modulus of water for each glass series
328 derived by extrapolation does depend on the anhydrous composition (Table 4), which is
329 also reported by previous studies (Malfait et al. 2011; Whingttington et al. 2012). As a
330 result, density models that assume ideal mixing of the water component
331 (composition-independent $\bar{V}_{H_2O}$) may result in larger uncertainties for the density of
332 hydrous melts at higher pressures. Under the assumption of an ideal mixing model, it is
333 now well established that the partial molar volumes of major oxide components are
334 independent of composition in anhydrous silicate melts (Lange and Carmchael 1987).
335 Schilling et al. (2001) suggested that the ideal mixing model is also applicable to elastic
336 properties and acoustic velocities of anhydrous glasses in the anorthite-diopside-forsterite
337 (An-Di-Fo) system. However, they cautioned that extrapolating molar elastic moduli to
338 drastically different compositions can lead to significant errors due to the different
339 structures. The reasoning behind this was further illustrated by the fact that the measured
340 elastic moduli for silica glass (K_S = 36.5 GPa, Bass 1995) are markedly different from the
341 inferred molar K_S (47.4 GPa) of a virtual SiO_2 component in the An-Di-Fo glasses
342 (Schilling et al. 2001). We speculate that the ideal mixing model may not apply to the
343 bulk modulus of hydrous glasses. Therefore, it seems that the partial molar K_S of water
344 depends on the anhydrous composition of the glasses, which is in contrast to $\bar{V}_{H_2O}$.

345 Nevertheless, the partial molar K_S of water for andesite and rhyolite melts (2.5 and

346 2.7 GPa, respectively) are independent of silicate composition at 1273 K (Malfait et al.
347 2014). This suggests that the behavior of water in melts and glasses may differ
348 significantly. This discrepancy is likely related to configurational contributions (unique to
349 melts) to the physical properties of melts (Richet and Neuville, 1992). In particular,
350 Stebbins et al. (1984) indicated that the ideal mixing model can be used to reproduce the
351 heat capacities of silicate glasses within error, but is less appropriate for that of silicate
352 melts due to the development of new structural configurations at temperatures above T_g.
353 Moreover, the effect of water speciation with temperature cannot be excluded. For
354 instance, the concentration of OH groups in the melt varies strongly with temperature and
355 is far greater than predicted by spectroscopic studies on glasses at ambient conditions
356 (Nowak and Behrens 1995). Consequently, there is a fundamental difference in the effect
357 of water on silicate melts versus glasses, systematic investigations are necessary to
358 understand the volumetric and elastic properties both in glasses and melts in the future.
359

360 **Water speciation**

361 The role of water in silicate glasses is directly linked to its speciation. It has long
362 been recognized that water dissolves in silicate glasses as hydroxyl groups (OH) and
363 molecular water (H_2O_{mol}) (Newman et al. 1986; Stolper 1982). As a traditional view,
364 hydroxyl groups predominate in silicate glasses at lower water content, while the fraction
365 of H_2O_{mol} increases with water content (Schmidt et al. 2001; Stolper 1982). The strongly

366 nonlinear role of water on the melt viscosity has been interpreted as the structural
367 consequences of the decreasing proportion of water dissolved as OH groups within the
368 melt with increasing water content (Stolper 1982). It appears that H_2O_{mol} does not affect
369 melt viscosity, and the amount of OH groups in the melt structure solely determines the
370 viscosity (Dingwell et al. 1996). Additionally, Richet and Polian (1998) found that the
371 variations of the shear modulus of hydrous andesite glasses are discontinuous with
372 increasing water content and ascribed it to rapidly increasing H_2O_{mol} concentration when
373 the total water content is above 1 wt%.

374 However, the molar volume, sound velocities, and elastic properties of the hydrous
375 silicate glasses from this study are all linear functions of water content. The same trends
376 were observed in a variety of glasses in previous studies (Malfait et al. 2011; Whittington
377 et al. 2012; Wu et al. 2017). Because we did not carry out spectroscopic measurements,
378 two possible interpretations can be proposed for the observations: (1) Water affects these
379 properties in the same manner regardless of its speciation because the linear trend was
380 observed in ranges where either OH groups or H_2O_{mol} predominate. The hydroxyl groups
381 dominate at low water contents before being overtaken by H_2O_{mol}, which occurs in
382 quenched glasses at water contents of 3-4 wt% (Stolper 1982). Therefore, the speciation
383 change of water has little effect on the volume or K_S, implying that the volume change of
384 the reaction between bridging oxygen and H_2O_{mol} to form OH is small in all glass series.
385 It further indicates that the changes in water speciation are driven by the entropy rather

than the volume of the system (Richet and Polian 1998). Moreover, Whittington et al. (2012) proposed that the effects of water on compression mechanisms are determined by water-silicate interactions, but not the interconversion of water speciation. (2) Like viscosity, the molar volume and elastic properties are sensitive to water speciation. Recently, Cody et al. (2020) used ^{1}H MAS nuclear magnetic resonance (NMR) spectroscopy to measure water speciation in aluminosilicate glasses. They suggested that H_2O_{mol} species are predominant over OH initially, while OH becomes dominant at very high total water content (>20 mol%). This recent finding is dramatically different from the traditional view of the water speciation trend. Thus, based on the new speciation trend, the linear correlation of the molar volume, wave velocities, and elastic properties with water content can be attributed to the relatively constant ratio of OH to H_2O_{mol} with no interconversion between the two water species in the range of water content (up to 5.45 wt% H_2O) in our glasses.

Implications for the dissolution mechanisms of water

The OH and H_2O_{mol} species behave in distinct ways within the silicate network of glasses and melts (Behrens et al. 2007). Consequently, not only the quantification of water speciation but also the understanding of the water dissolution mechanisms in the

This is the peer-reviewed, final accepted version for American Mineralogist, published by the Mineralogical Society of America.
The published version is subject to change. Cite as Authors (Year) Title. American Mineralogist, in press.
DOI: https://doi.org/10.2138/am-2022-8451. http://www.minsocam.org/

406 silicate structure is important. The composition of the silicate system affects the water
407 dissolution mechanism. Water prefers to be present as H_2O_{mol} that interacts with the
408 bridging oxygens to produce OH linked to tetrahedral cation (T-OH) in highly
409 polymerized melts and free hydroxyl groups (M-OH, OH species bonded only to
410 network-modifying cations) may also be present in strongly depolymerized melts (Cody
411 et al. 2005; Le Losq et al. 2015; Moretti et al. 2014; Mysen and Cody 2005; Xue and
412 Kanzaki 2004). In addition, NMR studies for silicate glasses demonstrated the dissolution
413 mechanisms of water in Al-bearing silicate networks are essentially similar to those in
414 Al-free systems, and multiple dissolution mechanisms for water are present
415 simultaneously (Malfait and Xue 2010; Xue and Kanzaki 2008).

416 Indirect evidence, such as the reduction in viscosity (Friedman et al. 1963; Giordano
417 et al. 2004; Hess and Dingwell 1996; Richet et al. 1996) and T_g (Giordano et al. 2005) as
418 water is incorporated into the melts, may reflect the structural change in the silicate
419 network. In particular, water is much more effective at reducing the viscosity of
420 polymerized melts than depolymerized ones (Whittington et al. 2000), which indicates
421 that the water dissolution mechanism may depend on composition. The Poisson's ratio (ν)
422 is a direct proxy for melt structure that correlates with network connectivity and is
423 expressed as $\nu = 1/2 \cdot [(V_P/V_S)^2 - 2]/[(V_P/V_S)^2 - 1]$. According to experimental
424 evidence, ν increases with rising atomic packing density (C_g) and decreases with
425 increasing average coordination number $\langle n \rangle$ or the number of bridging oxygen n_{BO}

426 (Greaves et al. 2011; Rouxel 2007). Hence, the increase in Poisson's ratio could be used
427 to qualitatively predict the network depolymerization. As might be expected, within
428 experimental errors, the Poisson's ratio for each glass series is a linear function of water
429 content (Fig. 7a). The increase of ν with the addition of H_2O together with the NMR
430 spectroscopic evidence for the formation of T-OH (T = Si, Al) through the rupture of
431 oxygen bridges: T-O-T +H_2O = 2T-OH (Farnan et al. 1987; Malfait and Xue 2010; Xue
432 2009; Xue and Kanzaki 2006), supports the hypothesis that dissolved water
433 depolymerizes melts in both Al-free (Nelson9) and Al-bearing (Nelson15 and NAS15)
434 silicate melts.

435 The Al/(Al + Si) ratio is one of the most important compositional variables of
436 natural magmatic systems. It has been proposed that the distribution of Al^{3+} among the
437 structural unit (Q^n, n = number of bridging oxygens to other tetrahedral) depends on the
438 Al/(Al + Si) of hydrous aluminosilicate systems (Mysen 2007). The Al^{3+} preferentially
439 occupies Q^4-species and the abundance of Q^4(4Al, i.e. the number of next-nearest Al to Si
440 is 4) increases rapidly with Al/(Al + Si), which plays a dominant role in raising the
441 fraction of Q^4-species with increasing bulk Al/(Al + Si) in peralkaline glasses and melts
442 (Mysen et al. 2003). In addition, dissolved water appears to exhibit preferences for
443 interaction with bridging oxygen bonds in Q^4-species (Mysen and Cody 2005; Zotov and
444 Keppler 1998).

445 The Poisson's ratio increases with H_2O at a higher rate in the Al-free Nelson9 series

This is the peer-reviewed, final accepted version for American Mineralogist, published by the Mineralogical Society of America.
The published version is subject to change. Cite as Authors (Year) Title. American Mineralogist, in press.
DOI: https://doi.org/10.2138/am-2022-8451. http://www.minsocam.org/

than in the other two Al-bearing systems (Fig. 7a, Table 4). Based on this behavior, we speculate that the water concentration derivative of Poisson's ratio ($\partial(v)/\partial(X_{H_2O})$) are possibly sensitive to the Al/(Al + Si) ratio. Fig. 7b shows that the $\partial(v)/\partial(X_{H_2O})$ is negatively correlated with Al/(Al + Si) when our data are plotted with previous data for rhyolite, phonolite, and trachyte glasses. The observation that $\partial(v)/\partial(X_{H_2O})$ decreases with increasing Al/(Al + Si) ratio may be explained by assuming that water prefers to interact with Si-O bonds to form Si-OH rather than Al-O bonds to produce Al-OH in peralkaline systems. This is a reasonable assumption because the rate of v-increase with water content ($\partial(v)/\partial(X_{H_2O})$), which represents the rate of depolymerization, decreases with increasing Al/(Al + Si) (therefore $Q^4(4Al)$ abundance). This implies that water interaction with Al-O bonds depolymerizes peralkaline silicate melts less effectively than with Si-O bonds. A recent NMR investigation revealed that the Al-OH/(Al-OH + Si-OH) proportion is smaller than the Al/(Al + Si) ratio in rhyolite and phonolite melts at lower temperatures (Malfait and Xue 2014). This also supports the idea that water prefers to form Si-OH rather than Al-OH in peralkaline silicate melts. Nevertheless, from the increased water solubility with Al/(Al + Si) observed by Holtz et al. (2000), Mysen and Richet (2019) hypothesized that water prefers to generate Al-OH rather than Si-OH for alkali meta-aluminosilicates. Moreover, the dependence of water solubility on composition has also been observed, particularly for peralkaline and peraluminous silicate composition (Behrens and Jantos 2001; Mysen and Armstrong 2002). Hence, the

466 dissolution mechanisms of water between peraluminous and peralkaline magma systems
467 might be different.

468 In summary, the decrease of water content derivative of the Poisson's ratio
469 ($\partial(v)/\partial(X_{H_2O})$) with increasing Al/(Al + Si) (Q^4(4Al) accordingly) indicates that water
470 interaction with Al-O bonds depolymerizes peralkaline silicate melts less effectively than
471 with Si-O bonds. Hence, we speculate that water prefers to interact with Si-O bonds
472 rather than Al-O bonds in peralkaline silicate systems. Further spectroscopic analyses are
473 required to obtain more detailed information on the speciation and dissolution
474 mechanisms of water. This study on the density, elastic properties of alkali-rich hydrous
475 silicate glasses could be the beginning of more comprehensive investigations on other
476 physical properties. Additional constraints at elevated *P*-*T* conditions are needed to
477 explore the effect of pressure and temperature on the structure and properties of hydrous
478 silicate melts/glasses, as well as to better understand the dynamic behavior of natural
479 magmas at depth.

480

481 **Acknowledgments**

482 We would like to thank Xiaoli Li for his support on microprobe analysis and Xinjian
483 Bao for technical assistance in the high pressure and high temperature laboratory at
484 Peking University. We thank George Morgan and Youxue Zhang for their helpful
485 suggestions on the conditions for electron microprobe analysis. We also wish to

acknowledge Wim Malfait and an anonymous reviewer for the constructive comments and Daniel Neuville for handling our manuscript. This study was supported by the National Natural Science Foundation of China (Grant Nos. 41672036 and 40972028).

REFERENCES CITED

Agee, C.B. (2008) Static compression of hydrous silicate melt and the effect of water on planetary differentiation. Earth and Planetary Science Letters, 265(3), 641-654.

Andreatch, P., and McSkimin, H.J. (1976) Pressure dependence of ultrasonic wave velocities and elastic stiffness moduli for a TiO_2-SiO_2 glass (Corning 7971). Journal of Applied Physics, 47(4), 1299-1301.

Ardia, P., Di Muro, A., Giordano, D., Massare, D., Sanchez-Valle, C., and Schmidt, M.W. (2014) Densification mechanisms of haplogranite glasses as a function of water content and pressure based on density and Raman data. Geochimica et Cosmochimica Acta, 138, 158.

Balzer, R., Behrens, H., Waurischk, T., Reinsch, S., Müller, R., Kiefer, P., Deubener, J., and Fechtelkord, M. (2020) Water in Alkali Aluminosilicate Glasses. Frontiers in Materials, 7.Bass, J.D. (1995) Elasticity of minerals, glasses, and melts. Mineral physics and crystallography: A handbook of physical constants, 2, 45-63.

Behrens, H. (1995) Determination of water solubilities in high-viscosity melts: An experimental study on $NaAlSi_3O_8$ and $KAlSi_3O_8$ melts. European Journal of Mineralogy, 7(4), 905-920.

Behrens, H. (2020) Water speciation in oxide glasses and melts. Chemical Geology, 558, 119850.

511 Behrens, H., and Jantos, N. (2001) The effect of anhydrous composition on water
512 solubility in granitic melts. American Mineralogist, 86(1-2), 14-20.
513 Behrens, H., Romano, C., Nowak, M., Holtz, F., and Dingwell, D.B. (1996) Near-infrared
514 spectroscopic determination of water species in glasses of the system $MAlSi_3O_8$
515 (M = Li, Na, K): an interlaboratory study. Chemical Geology, 128(1), 41-63.
516 Behrens, H., Zhang, Y., Leschik, M., Wiedenbeck, M., Heide, G., and Frischat, G.H.
517 (2007) Molecular H_2O as carrier for oxygen diffusion in hydrous silicate melts.
518 Earth and Planetary Science Letters, 254(1), 69-76.
519 Bouhifd, A.M., Whittington, A., Richet, P. (2001) Partial molar volume of water in
520 phonolitic glasses and liquids. Contributions to Mineralogy and Petrology, 142(2),
521 235-243.
522 Bouhifd, M.A., Whittington, A.G., and Richet, P. (2015) Densities and volumes of
523 hydrous silicate melts: New measurements and predictions. Chemical Geology,
524 418, 40-50.
525 Burnham, C.W., and Davis, N.F. (1971) The role of H_2O in silicate melts; I, P-V-T
526 relations in the system $NaAlSi_3O_8$-H_2O to 10 kilobars and 1000 °C. American
527 Journal of Science, 270(1), 54-79.
528 Cody, G.D., Ackerson, M., Beaumont, C., Foustoukos, D., Le Losq, C., and Mysen, B.O.
529 (2020) Revisiting water speciation in hydrous alumino-silicate glasses: A
530 discrepancy between solid-state ^1H NMR and NIR spectroscopy in the

determination of X-OH and H_2O. Geochimica et Cosmochimica Acta, 285, 150-174.

Cody, G.D., Mysen, B.O., and Lee, S.K. (2005) Structure vs. composition: A solid-state ^{1}H and ^{29}Si NMR study of quenched glasses along the Na_2O-SiO_2-H_2O join. Geochimica et Cosmochimica Acta, 69(9), 2373-2384.

Deschamps, T., Martinet, C., Bruneel, J.L., and Champagnon, B. (2011) Soda-lime silicate glass under hydrostatic pressure and indentation: a micro-Raman study. Journal of Physics: Condensed Matter, 23(3), 035402.

Dingwell, D.B., Romano, C., and Hess, K.U. (1996) The effect of water on the viscosity of a haplogranitic melt under P-T-X conditions relevant to silicic volcanism. Contributions to Mineralogy and Petrology, 124(1), 19-28.

Farnan, I., Kohn, S.C., and Dupree, R. (1987) A study of the structural role of water in hydrous silica glass using cross-polarisation magic angle spinning NMR. Geochimica et Cosmochimica Acta, 51(10), 2869-2873.

Giordano, D., Nichols, A.R.L., and Dingwell, D.B. (2005) Glass transition temperatures of natural hydrous melts: a relationship with shear viscosity and implications for the welding process. Journal of Volcanology and Geothermal Research, 142(1), 105-118.

Greaves, G.N., Greer, A.L., Lakes, R.S., and Rouxel, T. (2011) Poisson's ratio and modern materials. Nature Materials, 10(11), 823-837.

551 Gu, J.T., Fu, S., Gardner, J.E., Yamashita, S., Okuchi, T., and Lin, J.-F. (2021) Nonlinear
552 effects of hydration on high-pressure sound velocities of rhyolitic glasses.
553 American Mineralogist, 106(7), 1143-1152.
554 Hemley, R.J., Jephcoat, A.P., Mao, H.K., Zha, C.S., Finger, L.W., and Cox, D.E. (1987)
555 Static compression of H_2O-ice to 128 GPa (1.28 Mbar). Nature, 330(6150),
556 737-740.
557 Hess, K.U., and Dingwell, D.B. (1996) Viscosities of hydrous leucogranitic melts: A
558 non-Arrhenian model. American Mineralogist, 81(9-10), 1297-1300.
559 Holtz, F., Behrens, H., Dingwell, D.B., and Taylor, R.P. (1992) Water solubility in
560 aluminosilicate melts of haplogranite composition at 2 kbar. Chemical Geology,
561 96(3), 289-302.
562 Holtz, F., Roux, J., Behrens, H., and Pichavant, M. (2000) Water solubility in silica and
563 quartzofeldspathic melts. American Mineralogist, 85(5-6), 682-686.
564 Jing, Z., and Karato, S.-i. (2012) Effect of H_2O on the density of silicate melts at high
565 pressures: Static experiments and the application of a modified hard-sphere model
566 of equation of state. Geochimica et Cosmochimica Acta, 85, 357-372.
567 Lange, R.A. (1997) A revised model for the density and thermal expansivity of
568 K_2O-Na_2O-CaO-MgO-Al_2O_3-SiO_2 liquids from 700 to 1900 K: extension to
569 crustal magmatic temperatures. Contributions to Mineralogy and Petrology,
570 130(1), 1-11.
571 Le Losq, C., Dalou, C., and Mysen, B.O. (2017) In situ study at high pressure and

572 temperature of the environment of water in hydrous Na and Ca aluminosilicate
573 melts and coexisting aqueous fluids. Journal of Geophysical Research: Solid
574 Earth, 122(7), 4888-4899.
575 Le Losq, C., Mysen, B.O., and Cody, G.D. (2015) Water and magmas: insights about the
576 water solution mechanisms in alkali silicate melts from infrared, Raman, and ^{29}Si
577 solid-state NMR spectroscopies. Progress in Earth and Planetary Science, 2(1),
578 22.
579 Li, B., Chen, K., Kung, J., Liebermann, R.C., and Weidner, D.J. (2002) Sound velocity
580 measurement using transfer function method. Journal of Physics: Condensed
581 Matter, 14(44), 11337-11342.
582 Li, B., Kung, J., and Liebermann, R.C. (2004) Modern techniques in measuring elasticity
583 of Earth materials at high pressure and high temperature using ultrasonic
584 interferometry in conjunction with synchrotron X-radiation in multi-anvil
585 apparatus. Physics of the Earth and Planetary Interiors, 143-144, 559-574.
586 Li, B., and Liebermann, R.C. (2007) Indoor seismology by probing the Earths interior by
587 using sound velocity measurements at high pressures and temperatures.
588 Proceedings of the National Academy of Sciences, 104(22), 9145.
589 Li, B., and Liebermann, R.C. (2014) Study of the Earth's interior using measurements of
590 sound velocities in minerals by ultrasonic interferometry. Physics of the Earth and
591 Planetary Interiors, 233, 135-153.

592 Malfait, W.J., and Sanchez-Valle, C. (2013) Effect of water and network connectivity on
593 glass elasticity and melt fragility. Chemical Geology, 346, 72-80.
594 Malfait, W.J., Sanchez-Valle, C., Ardia, P., Médard, E., and Lerch, P. (2011) Amorphous
595 Materials: Properties, Structure, and Durability†: Compositional dependent
596 compressibility of dissolved water in silicate glasses. American Mineralogist,
597 96(8-9), 1402-1409.
598 Malfait, W.J., Seifert, R., Petitgirard, S., Mezouar, M., and Sanchez-Valle, C. (2014a) The
599 density of andesitic melts and the compressibility of dissolved water in silicate
600 melts at crustal and upper mantle conditions. Earth and Planetary Science Letters,
601 393, 31-38.
602 Malfait, W.J., Seifert, R., Petitgirard, S., Perrillat, J.-P., Mezouar, M., Ota, T., Nakamura,
603 E., Lerch, P., and Sanchez-Valle, C. (2014b) Supervolcano eruptions driven by
604 melt buoyancy in large silicic magma chambers. Nature Geoscience, 7(2),
605 122-125.
606 Malfait, W.J., and Xue, X. (2010a) The nature of hydroxyl groups in aluminosilicate
607 glasses: Quantifying Si–OH and Al–OH abundances along the SiO_2–$NaAlSiO_4$
608 join by ^{1}H, ^{27}Al–^{1}H and ^{29}Si–^{1}H NMR spectroscopy. Geochimica et
609 Cosmochimica Acta, 74(2), 719-737.
610 Malfait, W.J., and Xue, X. (2010b) The partial ^{1}H NMR spectra of Al–OH and molecular
611 H_2O in hydrous aluminosilicate glasses: Component-Resolved analysis of ^{27}Al–^{1}H

612 cross polarization and ^{1}H spin-echo MAS NMR spectra. Solid State Nuclear
613 Magnetic Resonance, 37(3), 60-68.
614 Malfait, W.J., and Xue, X. (2014) Hydroxyl speciation in felsic magmas. Geochimica et
615 Cosmochimica Acta, 140, 606-620.
616 Manghnani, M.H., Williams, Q., Matsui, T., Schultz, P.C., and Kurkjian, C.R. (2020)
617 Effects of Composition, Pressure, and Temperature on the Elastic Properties of
618 SiO_2–TiO_2 Glasses: An Integrated Ultrasonic and Brillouin Study. 10(5), 481.
619 Matsukage, K.N., Jing, Z., and Karato, S.-i. (2005) Density of hydrous silicate melt at the
620 conditions of Earth's deep upper mantle. Nature, 438(7067), 488-491.
621 Meister, R., Robertson, E.C., Werre, R.W., and Raspet, R. (1980) Elastic moduli of rock
622 glasses under pressure to 8 kilobars and geophysical implications. Journal of
623 Geophysical Research: Solid Earth, 85(B11), 6461-6470.
624 Moretti, R., Le Losq, C., and Neuville, D.R. (2014) The amphoteric behavior of water in
625 silicate melts from the point of view of their ionic-polymeric constitution.
626 Chemical Geology, 367, 23-33.
627 Morgan, G.B., and London, D. (1996) Optimizing the electron microprobe analysis of
628 hydrous alkali aluminosilicate glasses. American Mineralogist, 81(9-10),
629 1176-1185.
630 Morgan, G.B., VI, and London, D. (2005) Effect of current density on the electron
631 microprobe analysis of alkali aluminosilicate glasses. American Mineralogist,

632 90(7), 1131-1138.

633 Mysen, B., and Richet, P. (2019) Water Solution Mechanisms and Structure. In B. Mysen,
634 and P. Richet, Eds. Silicate Glasses and Melts (Second Edition), p. 541-580.
635 Elsevier.

636 Mysen, B.O. (2007) The solution behavior of H_2O in peralkaline aluminosilicate melts at
637 high pressure with implications for properties of hydrous melts. Geochimica et
638 Cosmochimica Acta, 71(7), 1820-1834.

639 Mysen, B.O., and Armstrong, L. (2002) Solubility behavior of alkali aluminosilicate
640 components in aqueous fluids and silicate melts at high pressure and temperature.
641 Geochimica et Cosmochimica Acta, 66(12), 2287-2297.

642 Mysen, B.O., and Cody, G.D. (2005) Solution mechanisms of H_2O in depolymerized
643 peralkaline melts. Geochimica et Cosmochimica Acta, 69(23), 5557-5566.

644 Mysen, B.O., Lucier, A., and Cody, G.D. (2003) The structural behavior of Al^{3+} in
645 peralkaline melts and glasses in the system Na_2O-Al_2O_3-SiO_2. American
646 Mineralogist, 88(11-12), 1668-1678.

647 Nelson, S.A., and Carmichael, I.S.E. (1979) Partial molar volumes of oxide components
648 in silicate liquids. Contributions to Mineralogy and Petrology, 71(2), 117-124.

649 Newman, S., Stolper, E.M., and Epstein, S. (1986) Measurement of water in rhyolitic
650 glasses; calibration of an infrared spectroscopic technique. American Mineralogist,
651 71(11-12), 1527-1541.

652 Nowak, M., and Behrens, H. (1995) The speciation of water in haplogranitic glasses and
653 melts determined by in situ near-infrared spectroscopy. Geochimica et
654 Cosmochimica Acta, 59(16), 3445-3450.
655 Nowak, M., and Behrens, H. (2001) Water in rhyolitic magmas: getting a grip on a
656 slippery problem. Earth and Planetary Science Letters, 184(2), 515-522.
657 Ochs, F.A., and Lange, R.A. (1997) The partial molar volume, thermal expansivity, and
658 compressibility of H_2O in $NaAlSi_3O_8$ liquid: new measurements and an internally
659 consistent model. Contributions to Mineralogy and Petrology, 129(2), 155-165.
660 Ochs, F.A., and Lange, R.A. (1999) The Density of Hydrous Magmatic Liquids. Science,
661 283(5406), 1314-1317.
662 Ohira, I., Ohtani, E., Sakai, T., Miyahara, M., Hirao, N., Ohishi, Y., and Nishijima, M.
663 (2014) Stability of a hydrous δ-phase, $AlOOH–MgSiO_2(OH)_2$, and a mechanism
664 for water transport into the base of lower mantle. Earth and Planetary Science
665 Letters, 401, 12-17.
666 Richet, P., Lejeune, A.-M., Holtz, F., and Roux, J. (1996) Water and the viscosity of
667 andesite melts. Chemical Geology, 128(1), 185-197.
668 Richet, P., and Polian, A. (1998) Water as a Dense Icelike Component in Silicate Glasses.
669 Science, 281(5375), 396-398.
670 Richet, P., Whittington, A., Holtz, F., Behrens, H., Ohlhorst, S., and Wilke, M. (2000)
671 Water and the density of silicate glasses. Contributions to Mineralogy and

672 Petrology, 138(4), 337-347.

673 Riebling, E.F. (1966) Structure of Sodium Aluminosilicate Melts Containing at Least 50
674 mole % SiO_2 at 1500°C. The Journal of Chemical Physics, 44(8), 2857-2865.

675 Romano, C., Dingwell, D.B., and Behrens, H. (1995) The temperature dependence of the
676 speciation of water in $NaAlSi_3O_8$-$KAlSi_3O_8$ melts: an application of fictive
677 temperatures derived from synthetic fluid-inclusions. Contributions to Mineralogy
678 and Petrology, 122(1), 1-10.

679 Rouxel, T. (2007) Elastic Properties and Short-to Medium-Range Order in Glasses.
680 Journal of the American Ceramic Society, 90(10), 3019-3039.

681 Sakamaki, T. (2017) Density of hydrous magma. Chemical Geology, 475, 135-139.

682 Sakamaki, T., Ohtani, E., Urakawa, S., Suzuki, A., and Katayama, Y. (2009)
683 Measurement of hydrous peridotite magma density at high pressure using the
684 X-ray absorption method. Earth and Planetary Science Letters, 287(3), 293-297.

685 Sakamaki, T., Suzuki, A., and Ohtani, E. (2006) Stability of hydrous melt at the base of
686 the Earth's upper mantle. Nature, 439(7073), 192-194.

687 Schilling, F.R., Hauser, M., Sinogeikin, S.V., and Bass, J.D. (2001) Compositional
688 dependence of elastic properties and density of glasses in the system
689 anorthite-diopside-forsterite. Contributions to Mineralogy Petrology, 141, 297.

690 Stebbins, J.F., Carmichael, I.S.E., and Moret, L.K. (1984) Heat capacities and entropies
691 of silicate liquids and glasses. Contributions to Mineralogy and Petrology, 86(2),

692 131-148.

693 Schmidt, B.C., Behrens, H., Riemer, T., Kappes, R., and Dupree, R. (2001) Quantitative
694 determination of water speciation in aluminosilicate glasses: a comparative NMR
695 and IR spectroscopic study. Chemical Geology, 174(1), 195-208.

696 Seifert, R., Malfait, W.J., Petitgirard, S., and Sanchez-Valle, C. (2013) Density of
697 phonolitic magmas and time scales of crystal fractionation in magma chambers.
698 Earth and Planetary Science Letters, 381, 12-20.

699 Stolper, E. (1982) Water in silicate glasses: An infrared spectroscopic study.
700 Contributions to Mineralogy and Petrology, 81(1), 1-17.

701 Thompson, G., Smith, I., and Malpas, J. (2001) Origin of oceanic phonolites by crystal
702 fractionation and the problem of the Daly gap: an example from Rarotonga.
703 Contributions to Mineralogy and Petrology, 142(3), 336-346.

704 Whittington, A., Richet, P., and Holtz, F. (2000) Water and the viscosity of depolymerized
705 aluminosilicate melts. Geochimica et Cosmochimica Acta, 64(21), 3725-3736.

706 Whittington, A., Richet, P., Linard, Y., and Holtz, F. (2001) The viscosity of hydrous
707 phonolites and trachytes. Chemical Geology, 174(1), 209-223.

708 Whittington, A.G., Richet, P., and Polian, A. (2012) Water and the compressibility of
709 silicate glasses: A Brillouin spectroscopic study. American Mineralogist, 97(2-3),
710 455-467.

711 Wu, L., Yang, D.-B., Liu, J.-X., Hu, B., Xie, H.-S., Li, F.-F., Yu, Y., Xu, W.-L., and Gao,

712 C.-X. (2017) A Brillouin scattering study of hydrous basaltic glasses: the effect of
713 H_2O on their elastic behavior and implications for the densities of basaltic melts.
714 Physics and Chemistry of Minerals, 44(6), 431-444.
715 Xue, X. (2009) Water speciation in hydrous silicate and aluminosilicate glasses: Direct
716 evidence from ^{29}Si-^{1}H and ^{27}Al-^{1}H double-resonance NMR. American
717 Mineralogist, 94(2-3), 395-398.
718 Xue, X., and Kanzaki, M. (2004) Dissolution mechanisms of water in depolymerized
719 silicate melts: Constraints from ^{1}H and ^{29}Si NMR spectroscopy and ab initio
720 calculations. Geochimica et Cosmochimica Acta, 68(24), 5027-5057.
721 Xue, X., and Kanzaki, M. (2006) Depolymerization effect of water in aluminosilicate
722 glasses: Direct evidence from ^{1}H-^{27}Al heteronuclear correlation NMR. American
723 Mineralogist, 91(11-12), 1922-1926.
724 Xue, X., and Kanzaki, M. (2008) Structure of hydrous aluminosilicate glasses along the
725 diopside–anorthite join: A comprehensive one- and two-dimensional ^{1}H and ^{27}Al
726 NMR study. Geochimica et Cosmochimica Acta, 72(9), 2331-2348.
727 Zotov, N., and Keppler, H. (1998) The influence of water on the structure of hydrous
728 sodium tetrasilicate glasses. American Mineralogist, 83(7-8), 823-834.
729

This is the peer-reviewed, final accepted version for American Mineralogist, published by the Mineralogical Society of America.
The published version is subject to change. Cite as Authors (Year) Title. American Mineralogist, in press.
DOI: https://doi.org/10.2138/am-2022-8451. http://www.minsocam.org/

730 **Figure captions:**

731 **Figure 1.** A schematic diagram shows the principle of travel time measurements
732 using the ultrasonic interferometric technique (modified after Li and Liebermann 2014).

733 **Figure 2.** (a) Received signals for andesite glass on the buffer rod; (b) Simulation of
734 the pulse-echo overlap (PEO) method.

735 **Figure 3.** The density of the three series of hydrous silicate glasses against water
736 content. The dashed lines are linear fits to our data.

737 **Figure 4.** The variation of (a) compressional and (b) shear wave velocities of the
738 three series of hydrous silicate glasses against water content. The dashed lines are linear
739 fits to our data.

740 **Figure 5.** (a) Adiabatic bulk and (b) shear modulus of silicate glasses against water
741 content. The data from this study are shown as solid symbols, the data of rhyolite glass
742 from Malfait et al. (2011) are shown as open circles, the data of phonolite and trachyte
743 from Whittington et al. (2012) are shown as open squares and triangles, respectively. The
744 dashed lines are linear fits to our data.

745 **Figure 6.** (a) Room-temperature molar volume of hydrous silicate glasses against
746 water content. The dashed lines are linear fits to our data. (b) The fitted dashed lines yield
747 the partial molar volume of water ($\bar{V}_{H_2O}$) as they intercept with the y-axis at 100% H_2O.
748 The constant $\bar{V}_{H_2O}$ (12 ± 0.5 cm^3/mol, Richet et al. 2000) is shown for a comparison.
749 Errors of measurements are smaller than the symbol size.

This is the peer-reviewed, final accepted version for American Mineralogist, published by the Mineralogical Society of America.
The published version is subject to change. Cite as Authors (Year) Title. American Mineralogist, in press.
DOI: https://doi.org/10.2138/am-2022-8451. http://www.minsocam.org/

750 **Figure 7.** (a) Variation of the Poisson's ratio with water content; (b) The relationship
751 between the water content derivative of Poisson's ratio ($\partial(v)/\partial(X_{H_2O})$) and Al/(Al + Si)
752 ratio; data taken from M11 (Malfait et al. 2011) and W12 (Whittington et al. 2012) are
753 also plotted as open symbols. The dashed line(s) in (a) are linear fits to our data and in (b)
754 is a linear fit to all the data.
755

This is the peer-reviewed, final accepted version for American Mineralogist, published by the Mineralogical Society of America.
The published version is subject to change. Cite as Authors (Year) Title. American Mineralogist, in press.
DOI: https://doi.org/10.2138/am-2022-8451. http://www.minsocam.org/

Table 1. Compositions (wt %) of the silicate glasses

Sample	SiO_2	Al_2O_3	MgO	CaO	Na_2O	K_2O	H_2O	Total	*g.f.w.*‡
Nelson9*	72.74		8.2			18.42		99.36	61.730
Nelson9-1	73.72		8.09			18.33	0.00†	100.14	61.731
Nelson9-2	71.24		7.92			18.26	2.02 (4)	99.44	58.904
Nelson9-3	71.15		7.69			18.18	2.92 (5)	99.94	57.767
Nelson9-4	70.53		7.53			17.72	4.05 (4)	99.83	56.287
Nelson9-6	69.30		7.79			17.35	5.45 (6)	99.89	54.445
Nelson15*	60.36	21.47			11.25	6.44		99.52	67.936
Nelson15-1	61.58	21.21			10.17	6.70	0.00†	99.66	67.882
Nelson15-2	60.98	21.06			10.14	6.36	1.12 (4)	99.65	65.800
Nelson15-3	60.53	20.84			9.94	6.21	2.22 (4)	99.74	63.880
Nelson15-4	59.83	20.52			9.75	6.73	2.82 (8)	99.66	62.978
NAS15*	46.89	23.06			29.88			99.83	67.060
NAS15-1	46.22	24.01			28.81		0.00†	99.05	67.394
NAS15-2	47.55	23.58			26.09		2.57 (6)	99.79	62.908
NAS15-3	46.34	23.21			26.44		3.39 (10)	99.38	61.586
Andesite	59.47	20.91	5.24	9.69	2.92	1.72	0.00†	99.96	63.954

† Nominal water content of dry samples, other H_2O contents were determined by KFT analysis.

‡ Gram formula weight calculated as $g.f.w. = \sum X_i M_i$, where X_i is the mole fraction of each oxide component, and M_i is the molecular weight of each oxide component

* Nominal composition of the anhydrous starting materials

This is the peer-reviewed, final accepted version for American Mineralogist, published by the Mineralogical Society of America.
The published version is subject to change. Cite as Authors (Year) Title. American Mineralogist, in press.
DOI: https://doi.org/10.2138/am-2022-8451. http://www.minsocam.org/

763 **Table 2.** Densities and sound velocities of fused silica and anhydrous andesite glasses

ρ (g/cm^3)	V_P (m/s)	V_S (m/s)	V_P Diff.%[§]	V_S Diff.%[§]	Reference
			fused silica		
2.203 (5)	5955 (13)	3746 (5)			This study[*]
2.202	5933	3764	-0.37	0.47	Andreatch and McSkimin (1976)[$]
2.204	5955 (5)	3763 (5)	0.00	0.44	Meister et al. (1980)[†]
2.2007	5947 (6)	3769 (4)	-0.14	0.60	Manghnani et al. (2020)[$]
			Andesite		
2.589 (13)	6344 (4)	3696 (5)			This study[*]
2.571	6152 (5)	3616 (5)	-3.03	-2.16	Meister et al. (1980)[†]
2.513	6240	3700	-1.64	0.11	Richet and Polian (1998)[‡]
2.536	6213 (10)	3689 (12)	-2.07	-0.19	Malfait et al. (2011)[‡]

764 Sound velocities were measured using different methods: [*] ultrasonic interferometry;
765 [$] pulse superposition; [†] ultrasonic phase comparison; [‡] Brillouin scattering.
766 [§] $V_{(P, S)}$ Diff.% corresponds to ($V_{(P, S)}$ (literature data) − $V_{(P, S)}$ (this study)) × 100/ $V_{(P, S)}$
767 (this study).

This is the peer-reviewed, final accepted version for American Mineralogist, published by the Mineralogical Society of America.
The published version is subject to change. Cite as Authors (Year) Title. American Mineralogist, in press.
DOI: https://doi.org/10.2138/am-2022-8451. http://www.minsocam.org/

768 **Table 3.** Densities, acoustic velocities, and elastic properties of the investigated silicate glasses

Sample	ρ (g/cm^3)	H_2O (mol	molar V (cm^3/mo	L (mm)	t_P (μs)	t_S (μs)	V_P (m/s)	V_S (m/s)	K_S (GPa)	β_S (10^{-2}GPa^{-1})	G (GPa)	v
Nelson9-1	2.417 (13)	0.00	25.54 (4)	3.791 (8)	1.3694 (3)	2.2940 (7)	5537 (12)	3305 (7)	38.9 (2)	2.57 (2)	26.4 (2)	0.223 (4)
Nelson9-2	2.409 (10)	6.64	24.45 (5)	6.622 (4)	2.4042 (5)	4.0788 (12)	5509 (4)	3247 (2)	39.2 (2)	2.55 (1)	25.4 (1)	0.234 (1)
Nelson9-3	2.396 (9)	9.37	24.11 (3)	4.018 (6)	1.4684 (10)	2.5114 (8)	5473 (9)	3200 (5)	39.1 (2)	2.56 (1)	24.5 (1)	0.240 (3)
Nelson9-4	2.380 (3)	12.68	23.65 (1)	5.128 (8)	1.8814 (5)	3.2348 (13)	5451 (9)	3171 (5)	38.8 (1)	2.58 (1)	23.9 (1)	0.244 (3)
Nelson9-6	2.377 (7)	16.58	22.9 (2)	2.219 (4)	0.8218 (10)	1.4310 (11)	5400 (12)	3101 (6)	38.8 (2)	2.58 (1)	22.9 (1)	0.254 (4)
Nelson15-1	2.459 (4)	0.00	27.61 (1)	3.33 (2)	1.1457 (9)	1.9117 (12)	5813 (6)	3484 (3)	43.3 (1)	2.31 (1)	29.8 (1)	0.220 (2)
Nelson15-2	2.448 (7)	4.09	26.88 (2)	1.086 (2)	0.3758 (11)	0.6302 (15)	5806 (20)	3462 (10)	43.4 (3)	2.30 (1)	29.4 (2)	0.224 (7)
Nelson15-3	2.436 (6)	7.89	26.22 (2)	3.515 (6)	1.2120 (7)	2.0417 (7)	5800 (10)	3443 (6)	43.4 (2)	2.30 (1)	28.9 (1)	0.228 (4)
Nelson15-4	2.429 (12)	9.89	25.92 (4)	3.245 (2)	1.1226 (10)	1.8958 (7)	5781 (6)	3423 (2)	43.2 (2)	2.31 (1)	28.5 (2)	0.230 (2)
NAS15-1	2.546 (12)	0.00	26.47 (4)	2.505 (12)	0.8644 (30)	1.5002 (28)	5796 (34)	3340 (17)	47.7 (4)	2.10 (2)	28.4 (3)	0.252 (12)
NAS15-2	2.516 (7)	8.99	25.00 (2)	3.996 (4)	1.375 (15)	2.4078 (15)	5812 (9)	3319 (4)	48.0 (1)	2.08 (1)	27.7 (1)	0.258 (3)
NAS15-3	2.500 (12)	11.66	24.63 (4)	1.784 (2)	0.6178 (18)	1.0912 (1)	5775 (18)	3270 (4)	47.8 (2)	2.10 (1)	26.7 (1)	0.264 (6)

769 Table 4. The water content derivatives of wave velocities and Poisson's ratio, the partial
770 molar bulk modulus of water, and NBO/T of the investigated glass series

Sample	NBO/T*	$\partial(V_P)/\partial(X_{H_2O})$	$\partial(V_S)/\partial(X_{H_2O})$	$\overline{K}_{S_{H_2O}}$	$\partial(v)/\partial(X_{H_2O}) \times 10^{-3}$
Nelson9	0.64	-8.2 (11)	-12.2 (10)	38.9 (3)	1.83 (1)
Nelson15	0.04	-2.8 (10)	-5.8 (6)	43.3 (1)	1.03 (9)
NAS15	0.37	-0.9 (29)	-5.0 (30)	47.7 (15)	0.99 (29)

771 * Calculated by NBO/T = (Na + K + 2Mg - Al)/(Si + Al) for the anhydrous compositions.
772

This is the peer-reviewed, final accepted version for American Mineralogist, published by the Mineralogical Society of America.
The published version is subject to change. Cite as Authors (Year) Title. American Mineralogist, in press.
DOI: https://doi.org/10.2138/am-2022-8451. http://www.minsocam.org/

773 Table 5. The partial molar volume of water and synthesis conditions of hydrous silicate
774 glasses

Sample	H_2O (wt%)	Pressure (GPa)	Temperature (°C)	$\bar{V}_{H_2O}$(cm^3/mol) #
		This study		
Nelson9	0-5.45	0.5	1234-1240	10.0 ± 0.5
Nelson15	0-2.82	0.5	1240-1250	10.6 ± 0.3
NAS15	0-3.39	0.5	1250	10.6 ± 0.4
		Ardia et al. (2014)		
Haplogranite	0.15-5.24	0.5	1000	11.23 ± 1.00
Haplogranite	0.15-5.24	1.0	1000	12.17 ± 1.00
Haplogranite	0.15-5.24	1.5	1000	12.82 ± 1.00
Haplogranite	0.15-5.24	2.5	1000	13.74 ± 1.00
		Balzer et al. (2020)		
NAS	0.02-7.90	0.5	1250-1600	11.8 ± 0.1
NKAS(2:1)	0.02-8.00	0.5	1250-1600	12.0 ± 0.1
NKAS(1:1)	0.01-7.96	0.5	1250-1600	12.1 ± 0.2
		Bouhifd et al. (2001, 2015)		
Albite[#]	0-5.2	0.2	1200	10.2 ± 0.5[*]
Tephrite[#]	0-3	0.2-0.3	1300	10.4 ± 0.5[*]
Trachyte[#]	0-5	0.2-0.3	1300	11.2 ± 0.8[*]
Foidite[#]	0.7-2.3	0.3	1300	10.3 ± 1.0[*]
Phonolite	0-4.72	0.2-0.3	1200-1300	11.0 ± 0.5[*]
		Malfait et al. (2011)		
Andesite	0-3.01	0.7	1400	13.9 ± 0.4
Basalt	0.05-4.40	0-0.20	1170-1290	12.0 ± 0.3
		Wu et al. (2017)		
Basalt (FX)[$]	0-4.01	1.0	1400	11.4 ± 0.5 (11.6 ± 0.8[*])
Basalt (FW)[$]	0-5.23	1.0	1400	11.2 ± 0.4 (10.9 ± 0.6[*])
Basalt (SHT)[$]	0-3.45	1.0	1400	10.3 ± 0.6 (11.5 ± 0.5[*])
Basalt (FX)	0-5.48	2.0	1400	9.2 ± 1.2
Basalt (FW)	0-6.82	2.0	1400	9.3 ± 1.0
Basalt (SHT)	0-4.48	2.0	1400	8.9 ± 1.5

775 # $\bar{V}_{H_2O}$ is derived by intercept method described in the text. This table only summarize the data on
776 hydrous silicate glasses collected after Richet et al. (2000).
777 * $\bar{V}_{H_2O}$ of relaxed glasses after relaxation during dilatometry measurements up to T_g

778 $ FX(Feixian), FW(Fuxin), and SHT(Sihetun) are three kinds of basaltic glasses from the North China
779 Craton (NCC).

780 **Figure 1.**

781

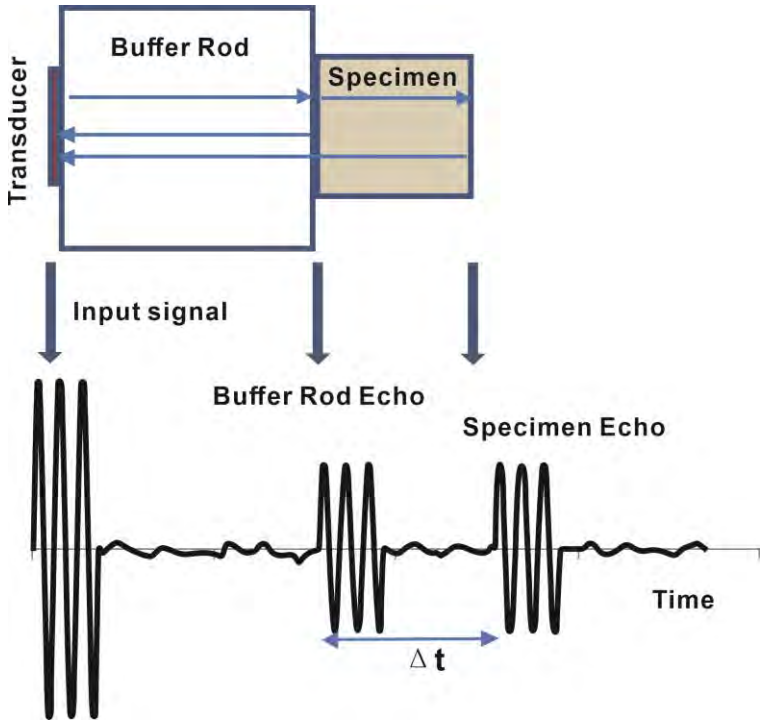

782

783

This is the peer-reviewed, final accepted version for American Mineralogist, published by the Mineralogical Society of America.
The published version is subject to change. Cite as Authors (Year) Title. American Mineralogist, in press.
DOI: https://doi.org/10.2138/am-2022-8451. http://www.minsocam.org/

784 **Figure 2.**

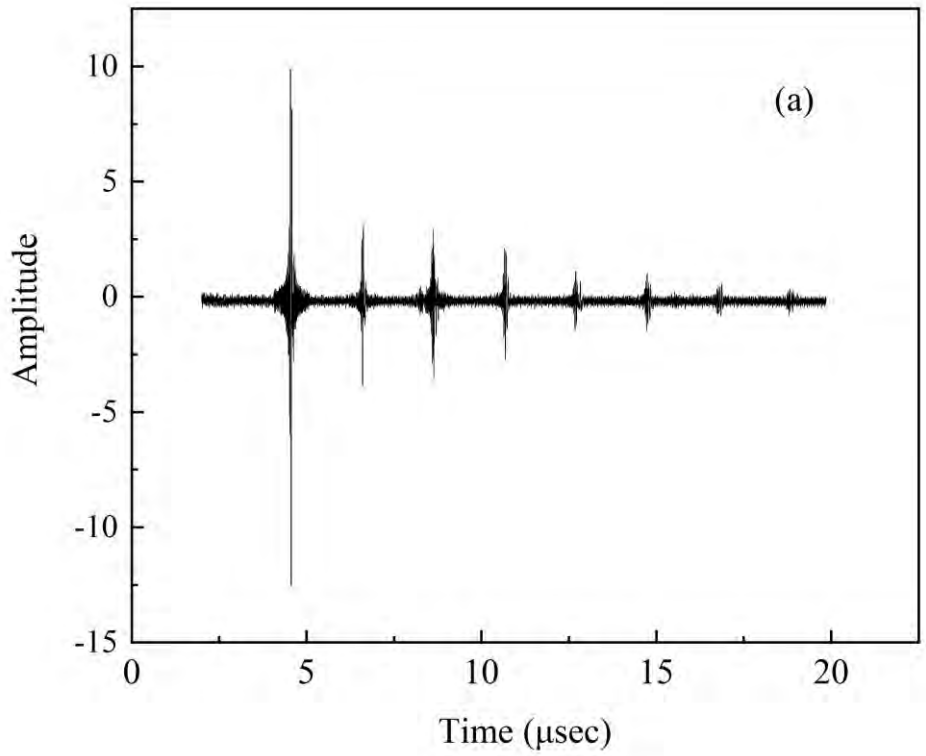

785

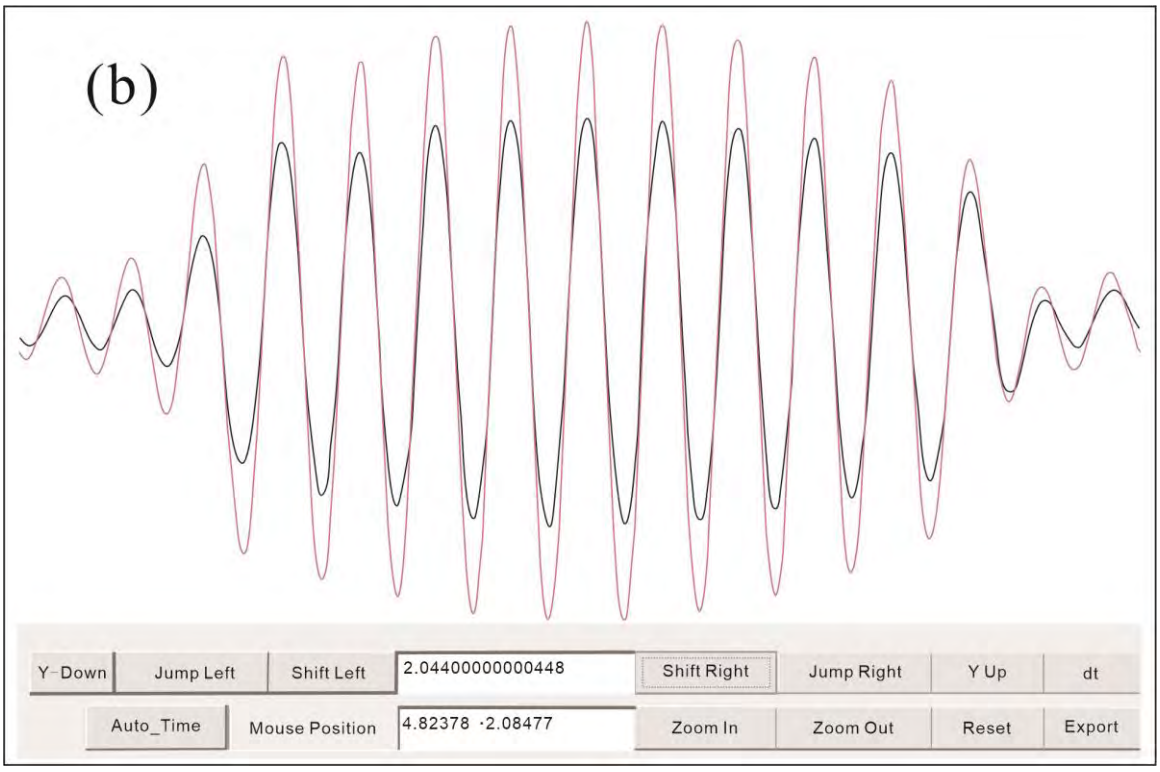

786

787

788 **Figure 3.**

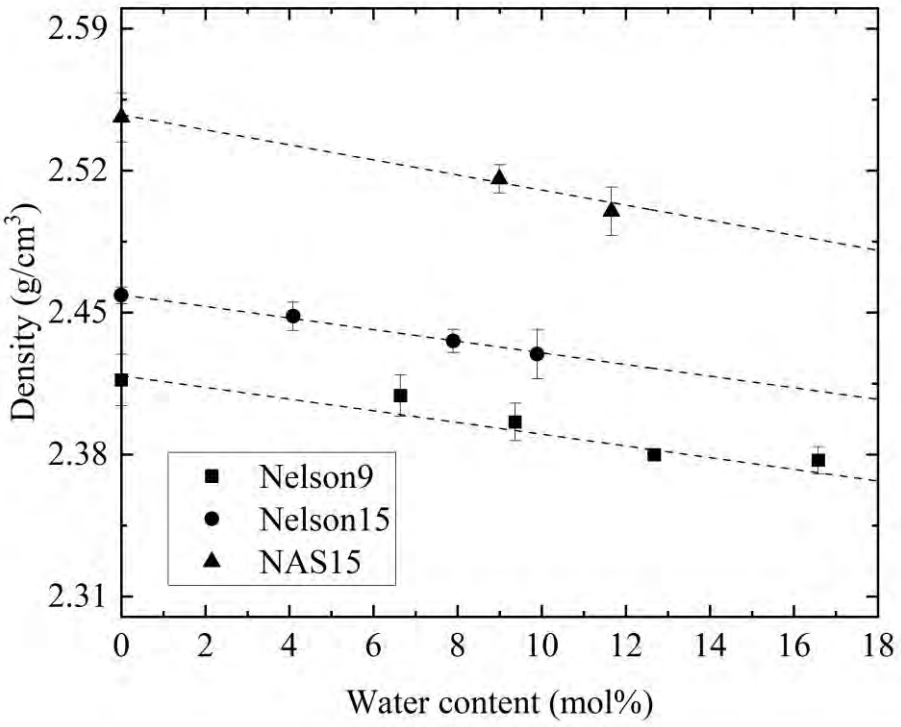

789

This is the peer-reviewed, final accepted version for American Mineralogist, published by the Mineralogical Society of America.
The published version is subject to change. Cite as Authors (Year) Title. American Mineralogist, in press.
DOI: https://doi.org/10.2138/am-2022-8451. http://www.minsocam.org/

790 **Figure 4.**

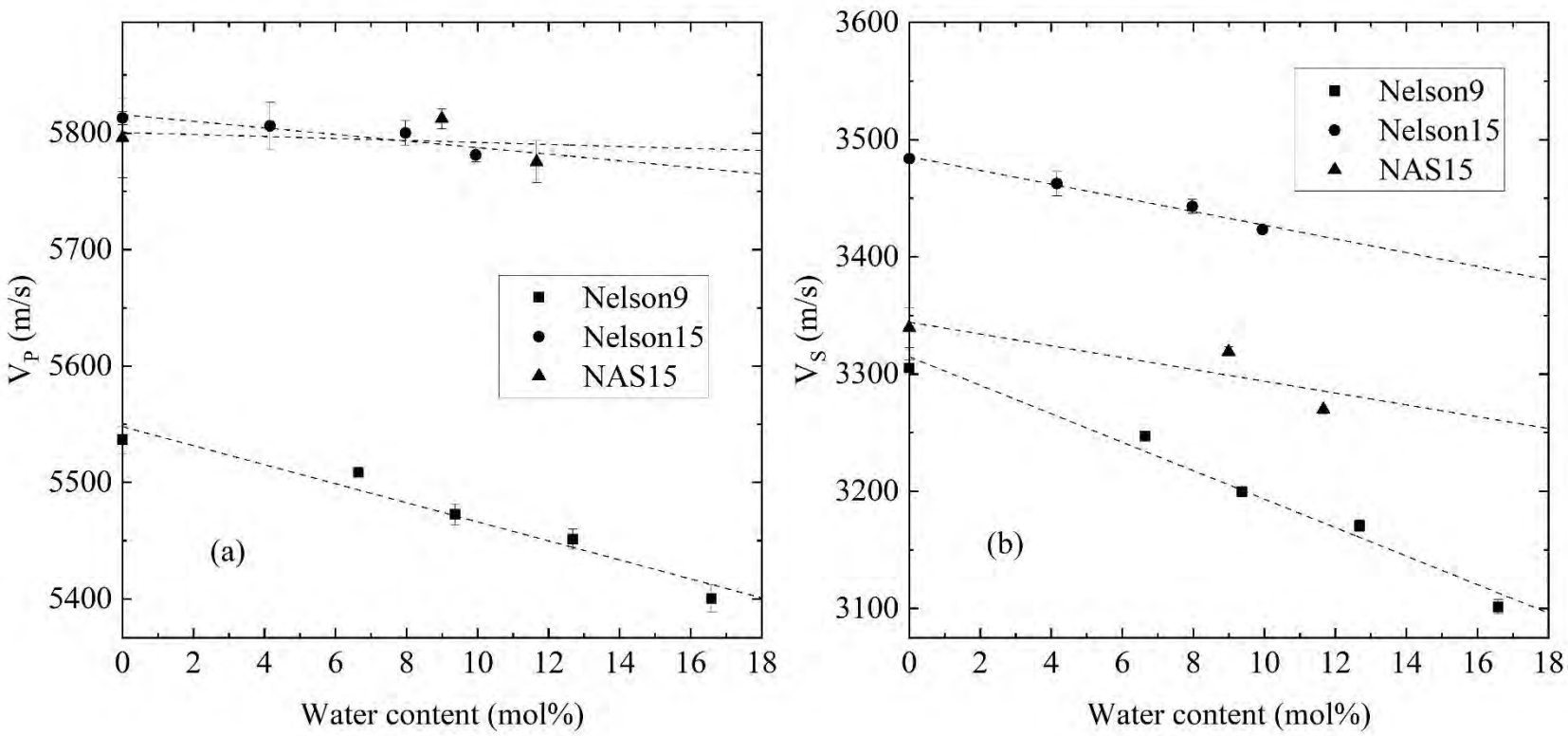

791

This is the peer-reviewed, final accepted version for American Mineralogist, published by the Mineralogical Society of America.
The published version is subject to change. Cite as Authors (Year) Title. American Mineralogist, in press.
DOI: https://doi.org/10.2138/am-2022-8451. http://www.minsocam.org/

792 **Figure 5.**

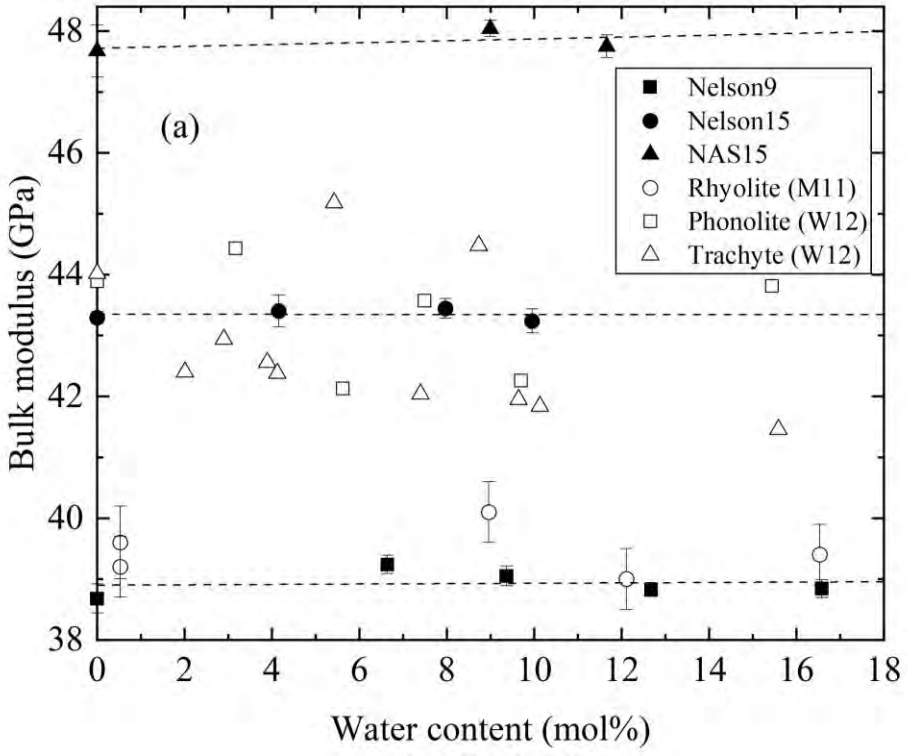

793

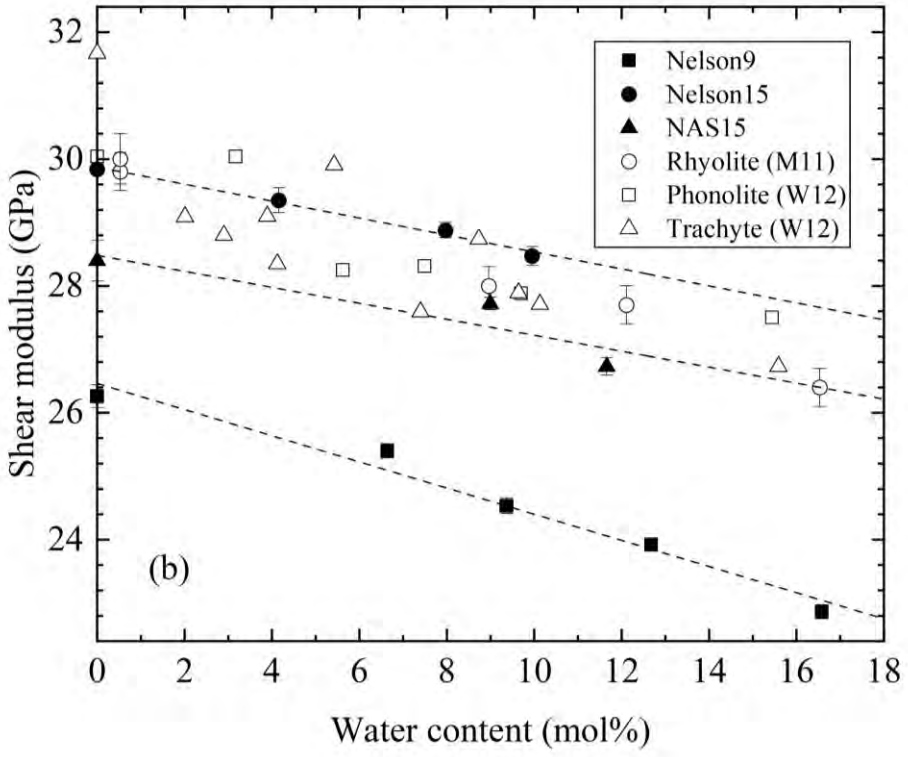

794

This is the peer-reviewed, final accepted version for American Mineralogist, published by the Mineralogical Society of America.
The published version is subject to change. Cite as Authors (Year) Title. American Mineralogist, in press.
DOI: https://doi.org/10.2138/am-2022-8451. http://www.minsocam.org/

795 **Figure 6.**

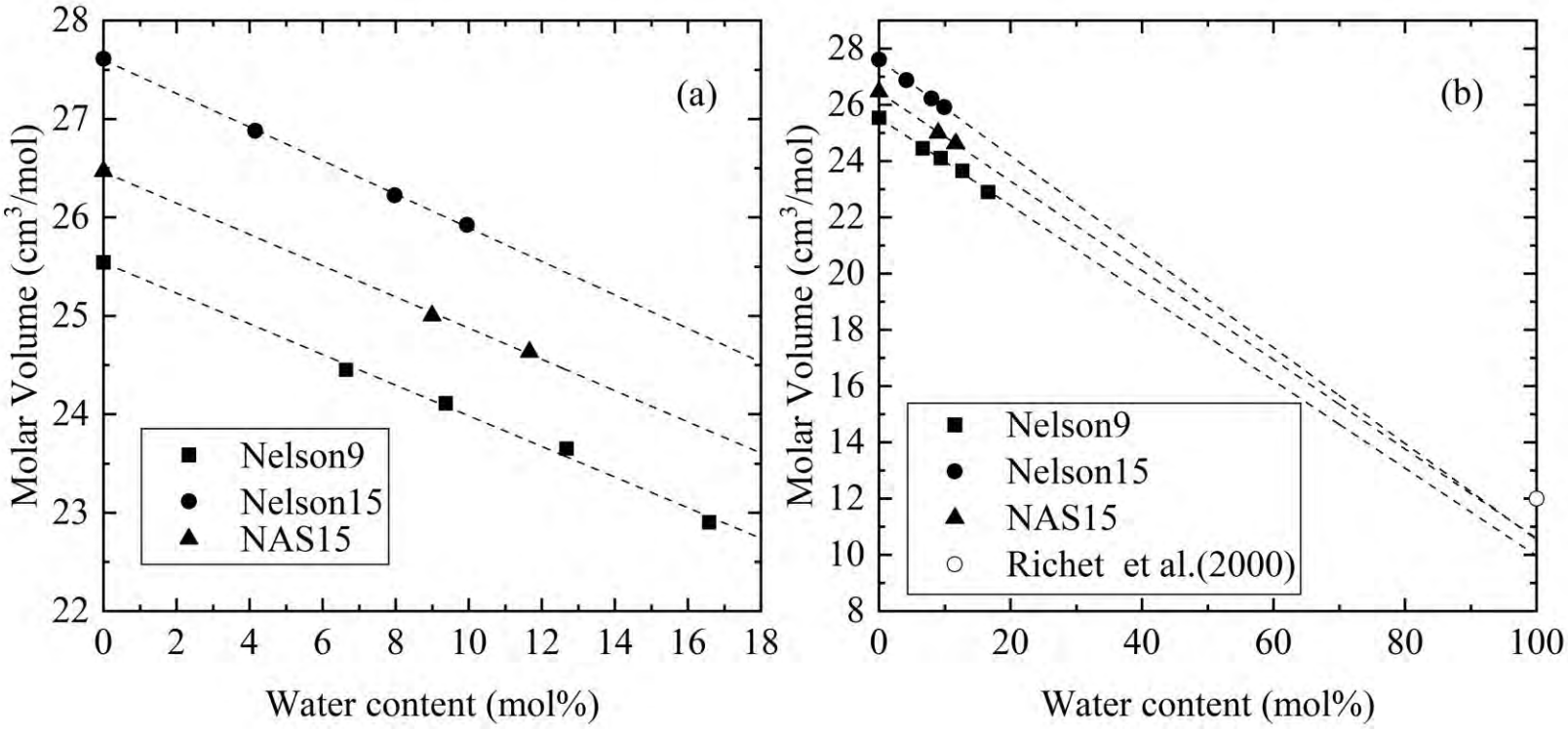

796

This is the peer-reviewed, final accepted version for American Mineralogist, published by the Mineralogical Society of America.
The published version is subject to change. Cite as Authors (Year) Title. American Mineralogist, in press.
DOI: https://doi.org/10.2138/am-2022-8451. http://www.minsocam.org/

797 **Figure 7.**

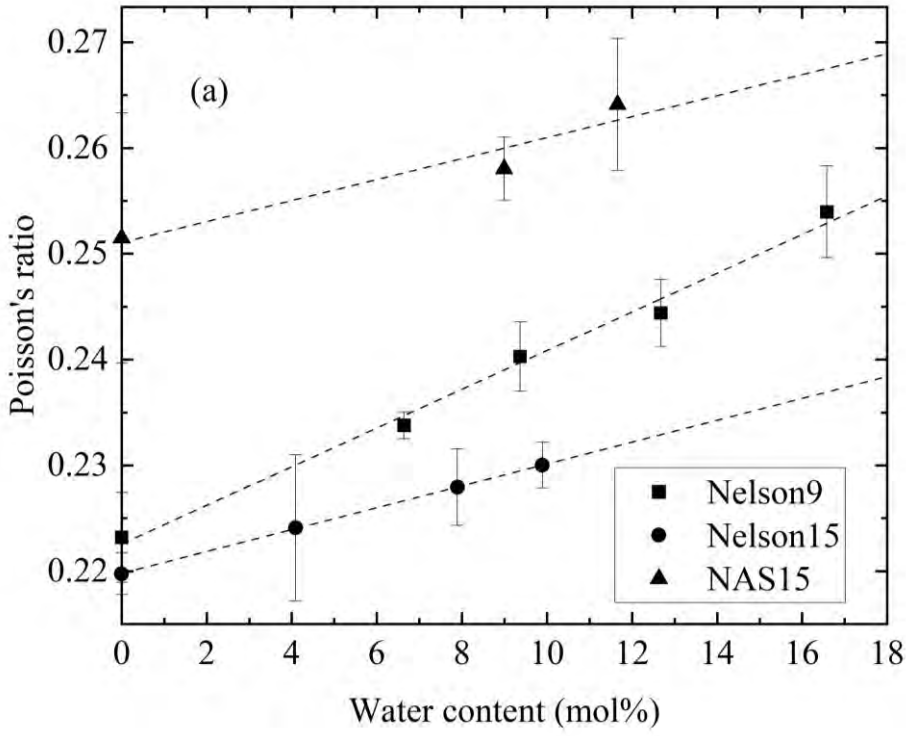

798

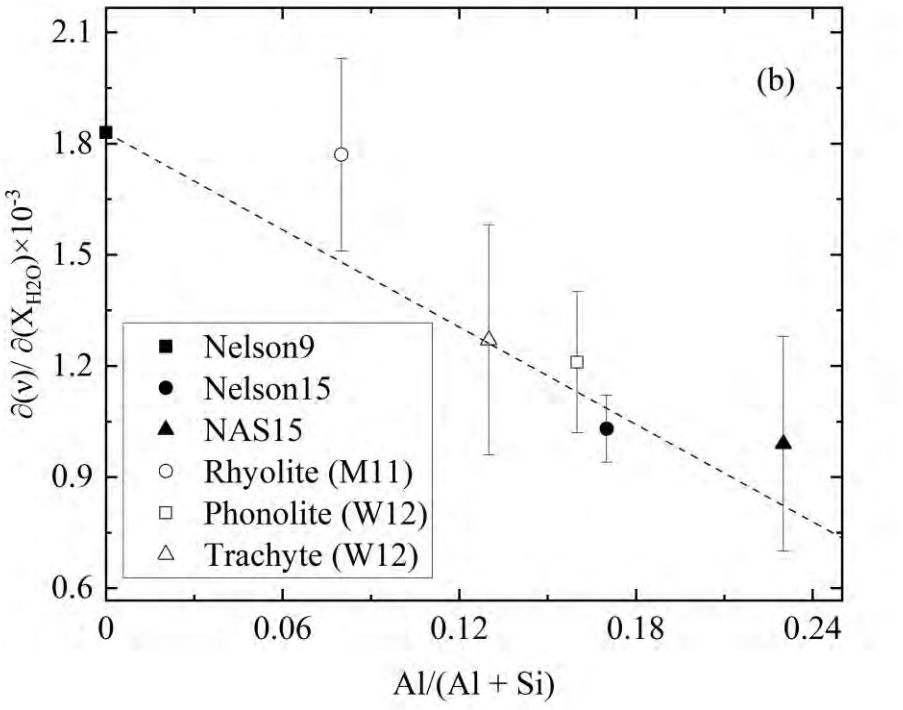

799